

Self-trapping of a binary Bose-Einstein condensate induced by interspecies interaction

S. K. Adhikari

Instituto de Física Teórica, UNESP - Universidade Estadual Paulista, 01.140-070 São Paulo, São Paulo, Brazil

Abstract.

The problem of self-trapping of a Bose-Einstein condensate (BEC) and a binary BEC in an optical lattice (OL) and double well (DW) is studied using the mean-field Gross-Pitaevskii equation. For both DW and OL, permanent self-trapping occurs in a window of the repulsive nonlinearity g of the GP equation: $g_{c1} < g < g_{c2}$. In case of OL, the critical nonlinearities g_{c1} and g_{c2} correspond to a window of chemical potentials $\mu_{c1} < \mu < \mu_{c2}$ defining the band gap(s) of the periodic OL. The permanent self-trapped BEC in an OL usually represents a breathing oscillation of a stable stationary gap soliton. The permanent self-trapped BEC in a DW, on the other hand, is a dynamically stabilized state without any stationary counterpart. For a binary BEC with intraspecies nonlinearities outside this window of nonlinearity, a permanent self trapping can be induced by tuning the interspecies interaction such that the effective nonlinearities of the components fall in the above window.

PACS numbers: 03.75.Lm, 03.75Kk, 03.75.Mn

1. Introduction

After the experimental observation of a Bose-Einstein condensate (BEC), it is realized that a quasi one-dimensional (1D) cigar-shaped trap [1] is convenient to study many novel and complex phenomena. In a cigar-shaped BEC, apart from a harmonic trap, double well (DW) [2], periodic optical-lattice (OL) [3], and quasi-periodic bichromatic OL [4] traps have been used. Usually, a repulsive BEC is localized in laboratory in an infinite trap. However, several other types of counter-intuitive localization of a repulsive BEC in a trap of finite height, where possible Josephson tunneling [2, 5, 6] of quantum fluids through barriers of finite height is expected to lead to delocalization, have lately drawn much attention. Of these, self trapping or localization of a repulsive BEC predominantly in one site of a DW [7, 8, 9, 10, 11], triple well [12] and OL [2, 13, 14, 15] potential has been the subject matter of many investigations. Macroscopic self trapping of a BEC was first predicted theoretically [6, 7, 16] and then observed experimentally [2, 5]. It is generally believed that self trapping is an intrinsic *dynamical* phenomenon, without any stationary counterpart. In this connection we note that the Anderson localization [4, 17] in a quasi-periodic or random potential and a gap [18] soliton in a periodic potential are both *stationary* states of the system. In the present critical study of self trapping in DW and OL potentials we find that, although, in the former case, is is a *dynamical* phenomenon, in the latter case, contrary to general belief, localization takes place in a *stationary* gap soliton state. There is no symmetry broken stationary state corresponding to the self-trapped state in DW.

To understand the self trapping in an OL and a DW potential, we perform extensive numerical simulation of self trapping of a BEC using the solution of the Gross-Pitaevskii (GP) equation. In our study, we find a striking similarity between self trappings in OL and DW. Both occur in a window of repulsive nonlinearity g of the GP equation: $g_{c1} < g < g_{c2}$. The numerical values of g_{c1} and g_{c2} depend on the respective trap parameters. (The existence of the upper limit of nonlinearity g_{c2} was never noted in previous studies.)

Although, the self trapping of a repulsive BEC in a DW represents a relatively simple mathematical problem, well described by the analytic two-mode model [7, 11], the self trapping of a repulsive BEC in a periodic OL involving an infinite number of wells, on the other hand, poses a formidable mathematical problem and the fundamental mechanism in this case is not well understood. For a repulsive BEC in an OL, one has localized gap-soliton states [3, 18, 19, 20]. We demonstrate that, in an OL, self trapping represents a permanent breathing oscillation of a stable stationary gap soliton. For self trapping in OL, we consider compact state(s) localized mostly on a single site of OL, in contrast to previous considerations of self trapping on multiple OL sites [13, 14, 21]. In the case of an OL, the critical nonlinearities g_{c1} and g_{c2} for self trapping define the window of chemical potentials corresponding to the band gap(s).

We also consider the self trapping of a binary BEC in OL and DW with tunable interspecies interaction near a Feshbach resonance [22]. For zero interspecies interaction,

self trapping takes place if the nonlinearities $g_i, i = 1, 2$ of the components are in the window $g_{c1} < g_i < g_{c2}$, and there is no self trapping if g_i 's are outside this window. In the presence of interspecies interaction, the effective nonlinearity of both components (arising from a combination of inter and intraspecies interactions) should lie in the above window for self trapping. When both $g_1, g_2 > g_{c2}$, for zero interspecies interaction there is no self trapping. We illustrate, using the solution of the GP equation, that, for both OL and DW, if g_{12} has an adequate attractive (negative) value, the effective nonlinearity of each component is reduced and one could have permanent self trapping. When both $g_1, g_2 < g_{c2}$, for zero interspecies interaction there is no self trapping. In this case, an appropriate repulsive (positive) interspecies nonlinearity can lead to effective nonlinearities of the components in the above window, and hence result in permanent self trapping.

2. Analytical formulation for Double-Well (DW) potential

We consider a binary cigar-shaped BEC in a DW. Atoms of both species (in two different hyperfine states) are assumed to have mass m and number N and the DW acts in the axial \hat{x} direction. Starting with the system of coupled 3D GP equations of the binary BEC one can reduce them to the following (dimensionless) 1D equations [23]:

$$\begin{aligned} i\dot{\phi}_i(x, t) = & -\frac{[\phi_i(x, t)]_{xx}}{2} + g_i|\phi_i(x, t)|^2\phi_i(x, t) \\ & + g_{12}|\phi_j(x, t)|^2\phi_i(x, t) + V(x)\phi_i(x, t), \end{aligned} \quad (1)$$

where $i \neq j = 1, 2$ denote the species, and wave functions ϕ_i are normalized as $\int_{-\infty}^{\infty} |\phi_i(x, t)|^2 dx = 1$. The suffix x denotes space derivatives and overhead dot time derivatives. In (1), time t , space x , nonlinearities g_i and g_{12} are related to the physical observables by [27]: $t = \omega_x t_{\text{phys}}$, $x = \hat{x}/l$, $\{g_i, g_{12}\} = 2\{a, a_{12}\}\lambda/l$ with $l = \sqrt{\hbar/m\omega_x}$ and $\lambda = \omega_\rho/\omega_x$ is the trap aspect ratio with ω_x and ω_ρ axial and radial (ρ) frequencies and where a_i and a_{12} are intraspecies and interspecies scattering lengths. The DW is taken as [9]

$$V(x) = x^2/2 + Ae^{-\kappa x^2}. \quad (2)$$

For a single-species BEC, the reduced 1D equation is

$$i\dot{\phi}(x, t) = -(1/2)\phi_{xx}(x, t) + g|\phi(x, t)|^2\phi(x, t) + V(x)\phi(x, t). \quad (3)$$

In the two-mode model [7, 11] a single-channel BEC wave function $\phi(x, t)$ of (3) is decomposed as [7]

$$\phi(x, t) = \psi_1(t)\Phi_1(x) + \psi_2(t)\Phi_2(x), \quad (4)$$

where spatial modes $\Phi_i(x) (i = 1, 2)$ in the two wells are orthonormalized as $\int \Phi_i(x)\Phi_j(x) = \delta_{ij}$ and the functions $\psi_i(t)$ satisfy $|\psi_1(t)|^2 + |\psi_2(t)|^2 = 1$. The functions $\psi_i(t)$ are complex and are separated into its real and imaginary parts as $\psi_i(t) = |\psi_i(t)| \exp(i\theta_i)$. A population imbalance

$$S(t) \equiv (|\psi_1(t)|^2 - |\psi_2(t)|^2) / (|\psi_1(t)|^2 + |\psi_2(t)|^2) = (|\psi_1(t)|^2 - |\psi_2(t)|^2) \quad (5)$$

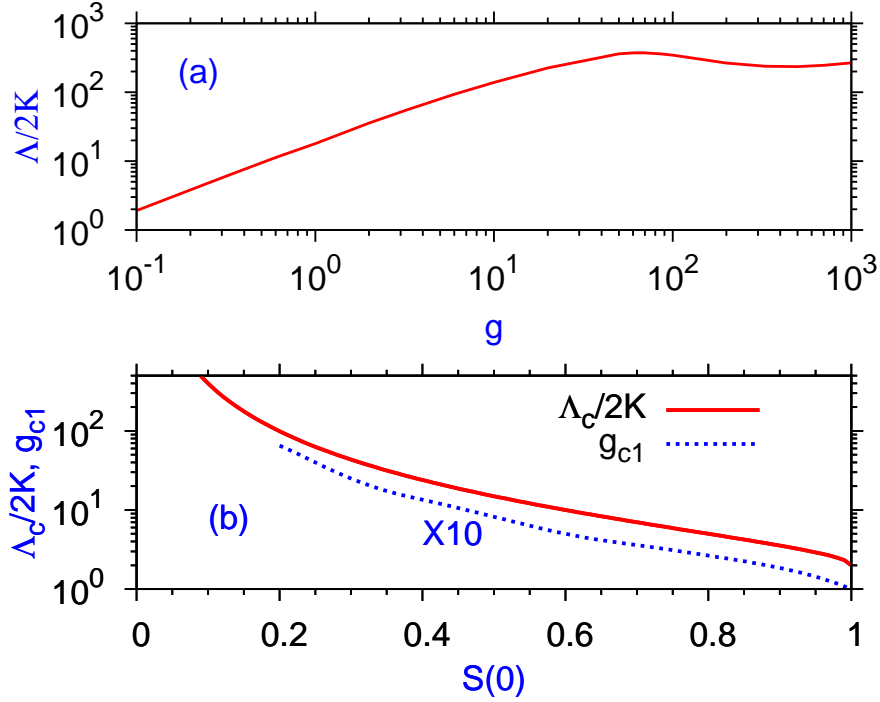


Figure 1. (a) The function $\Lambda/2K$ versus g obtained using two-mode functions (10). (b) The critical $\Lambda_c/2K$ and g_{c1} versus $S(0)$ from (9) and (10) for $\theta(0) = 0$.

and phase difference $\theta \equiv \theta_2 - \theta_1$ then serve as a pair of conjugate variables. The approximation (4) is then substituted in (3), and after some straightforward algebra we obtain [7]

$$\dot{S}(t) = -2K\sqrt{1 - S^2(t)}\sin\theta(t), \quad (6)$$

$$\dot{\theta}(t) = \Lambda S(t) + 2K\frac{S(t)}{\sqrt{1 - S^2(t)}}\cos\theta(t), \quad (7)$$

where $\Lambda = g \int dx \Phi_i^4(x)$ and

$$K = - \int dx \Phi_1(x) \left[-\frac{1}{2} \frac{d^2}{dx^2} + V(x) \right] \Phi_2(x). \quad (8)$$

The two-mode equations (6) and (7) are the Hamilton equations [7] $\dot{S} = -\partial H/\partial\theta$, $\dot{\theta} = -\partial H/\partial S$, for Hamiltonian $H = \Lambda S^2(t)/2 - 2K\sqrt{1 - S^2(t)}\cos\theta(t)$. The transition from Josephson oscillation to self trapping happens at $H = 2K$ above a critical $\Lambda = \Lambda_c$ for [7]

$$\frac{\Lambda}{2K} > \frac{\Lambda_c}{2K} \equiv \frac{2 + 2\sqrt{1 - S^2(0)}\cos\theta(0)}{S^2(0)}. \quad (9)$$

To perform a numerical calculation using the two-mode model we choose the mode functions as [7]

$$\Phi_{1,2}(x) = [\Phi_+(x) \pm \Phi_-(x)]/\sqrt{2}, \quad (10)$$

with the property $\Phi_1(-x) = \Phi_2(x)$, where $\Phi_{\pm}(x)$ are the symmetric ground and antisymmetric first excited state of (3) with potential (2) with an appropriate g . The parameters of potential (2) are taken as $A = 16$ and $\kappa = 10$ (used in most of numerical calculations below).

Now we calculate the quantity $\Lambda/2K$ for different g and plot in figure 1 (a). Then a critical Λ_c for self trapping is obtained from (9) and plotted in figure 1 (b) versus $S(0)$ for $\theta(0) = 0$. From figure 1 (b) we see that for $S(0) = 0.1$, the critical $\Lambda_c/2K \sim 400$. From figure 1 (a) we see that this $\Lambda/2K$ is never attained for any nonlinearity g . Hence no self trapping can be obtained for $S(0) < 0.1$. For $S(0) > 0.2$, the critical $\Lambda_c/2K$ for self trapping as obtained from figure 1 (b), can be attained for $g > g_{1c}$ as seen in figure 1 (a). However, with further increase of g , Λ continues to be always greater than Λ_c and the self trapping is never destroyed with the increase of g . In our numerical study we shall find that the self trapping is destroyed with the increase of g . This is reasonable as the two-mode model with the neglect of overlap integrals between the mode functions $\Phi_{1,2}(x)$ is expected to be valid for small g only. A critical nonlinearity for self trapping g_{1c} for $\theta(0) = 0$ and different $S(0)$ is then obtained from the results of $\Lambda/2K - g$ and $\Lambda_c/2K - S(0)$ plots in figures 1 (a) and (b) and is also plotted in figure 1 (b).

3. Numerical results for Double-Well (DW) potential

The GP equations are solved numerically using the Crank-Nicolson scheme [27, 28] with space and time steps 0.025 and 0.0002, respectively, by real-time propagation with FORTRAN programs provided in [27].

3.1. Single-Channel BEC

Here we consider DW (2) with $A = 16$ and $\kappa = 10$, as in some previous studies [9, 10] on self trapping. In numerical simulation we create an initial state with a fixed population imbalance $S(0)$, by looking for the ground state at $x = x_0$ of the following asymmetric well [9]

$$U(x) = (x - x_0)^2/2 + Ae^{-\kappa x^2}. \quad (11)$$

The initial $S(0)$ is achieved by varying the parameter x_0 in (11) [9]. Once this initial state is created, x_0 is reduced to zero so that DW (11) reduces to DW (2) with $x_0 = 0$. If x_0 is reduced slowly during time evolution, the initial asymmetric state relaxes to a symmetric stationary state of DW (2) and there is no self trapping. On the other hand if x_0 is reduced quickly, there is always self trapping provided that g lies in the appropriate window: $g_{1c} < g < g_{2c}$. This is shown in figure 2, where we plot the density at different t after x_0 is reduced to zero during an interval $\Delta t = 5$, and 20. From figure 2 we find that there is self trapping for $\Delta t = 5$ and no self trapping for $\Delta t = 20$, when the asymmetric initial state relaxes to a final symmetric state. By actual substitution of the wave function of the self-trapped state in the *time-independent* GP equation we verify that there is no stationary state of the DW with this density. The present trapped

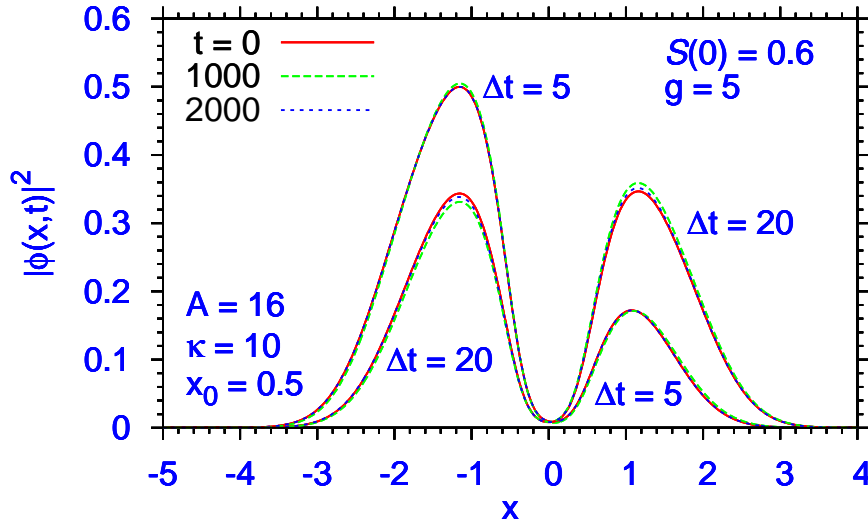


Figure 2. Density $|\phi(x,t)|^2$ versus x at different t when an initial state, created as the ground state of the asymmetric DW (11), is allowed to evolve in time while the asymmetric DW (11) is changed to the symmetric DW (2) by reducing x_0 to zero slowly in an interval of time $\Delta t = 5, 20$. When the transition is quick ($\Delta t = 5$) a permanent self trapping with an asymmetric profile emerges. For a slow transition ($\Delta t = 20$), the system smoothly moves to the symmetric ground state of the symmetric DW (2) and there is no self trapping.

wave function was generated from the ground state of DW (11) and is always positive with no node and the present self trapping is dynamical without any static counterpart.

The self trapping is sensitive to $S(0)$. There is no self trapping for a small $S(0) (< 0.1)$ (viz., two-mode model of section 2). In figure 3 (a) (upper panel) we plot $S(t)$ versus t to illustrate the trapping and oscillation for different g ($= 1, 10, 100, 1000$) for $S(0) = 0.3$. For $g = 1$, there is Josephson oscillation with $\langle S(t) \rangle = 0$. For $g = 10$ we have $\langle S(t) \rangle \sim 0.3$ insuring self trapping. As g is further increased, the nonlinear term in the GP equation becomes much larger than the Gaussian wall $A \exp(-\kappa x^2)$ in (2). Consequently, the DW appears like a single well and classical center-of-mass oscillation appears for a large g . For $g = 100$ the oscillation is irregular because the Gaussian wall is not fully negligible. Finally, for $g = 1000$ the Gaussian wall can be completely neglected and we have clean classical center-of-mass oscillation. The $S(t)$ versus t plot for $S(0) = 0.3$ and $g = 10$ at large times is shown in the lower panel of figure 3 (a), where self trapping is confirmed up to $t = 5000$ – an interval much larger than tunneling time which is at best ~ 100 . The evolution of $S(t)$ at large times $S(\infty)$ for different $S(0)$ as g is increased is shown in figure 3 (b). A nonzero $S(\infty)$ ensures self trapping, which appears in the window: $g_{c1} < g < g_{c2}$. The prediction of the analytical two-mode model of section 2, from figure 1 (b), for g_{c1} are shown by arrows in figure 3 (b) for $S(0) = 0.3$ and 0.6 in good agreement with numerical simulation. It is noted that in all calculations reported here $g_{c2} < 100$ – a medium value of nonlinearity where the mean-field GP description is well justified. For larger values of nonlinearities,

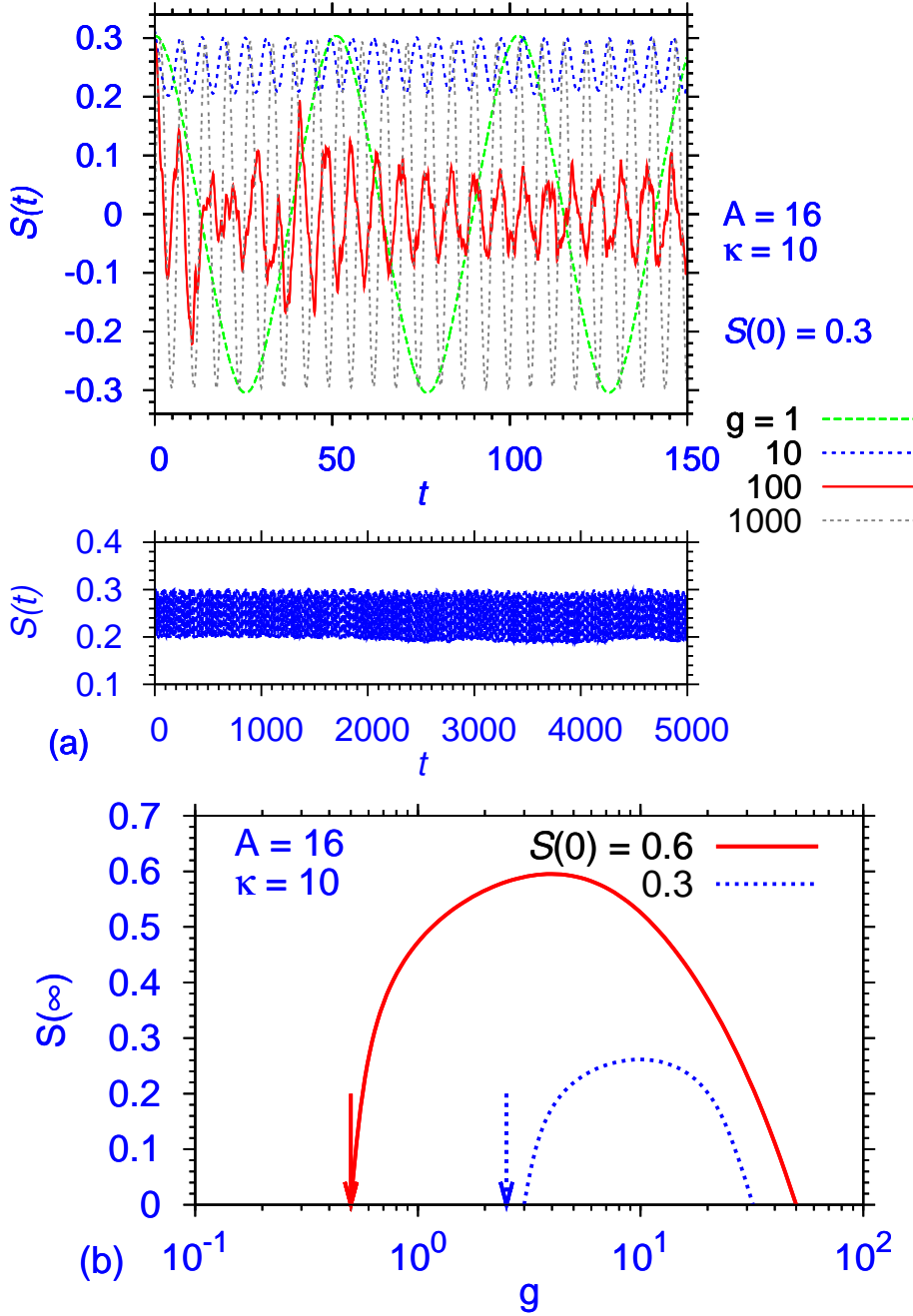


Figure 3. (a) (upper panel) Population imbalance $S(t)$ versus t for $S(0) = 0.3$ in DW (2). (lower panel) Long-time $S(t)$ versus t for $g = 10$. (b) Average population imbalance at large time $S(\infty)$ versus g for $S(0) = 0.3$ and 0.6 . The arrows are results for g_{c1} from figure 1 (b).

beyond mean-field corrections to the GP equation [29] could be relevant [30]. However, we expect the general conclusions of this study to remain valid for the present set of parameters.

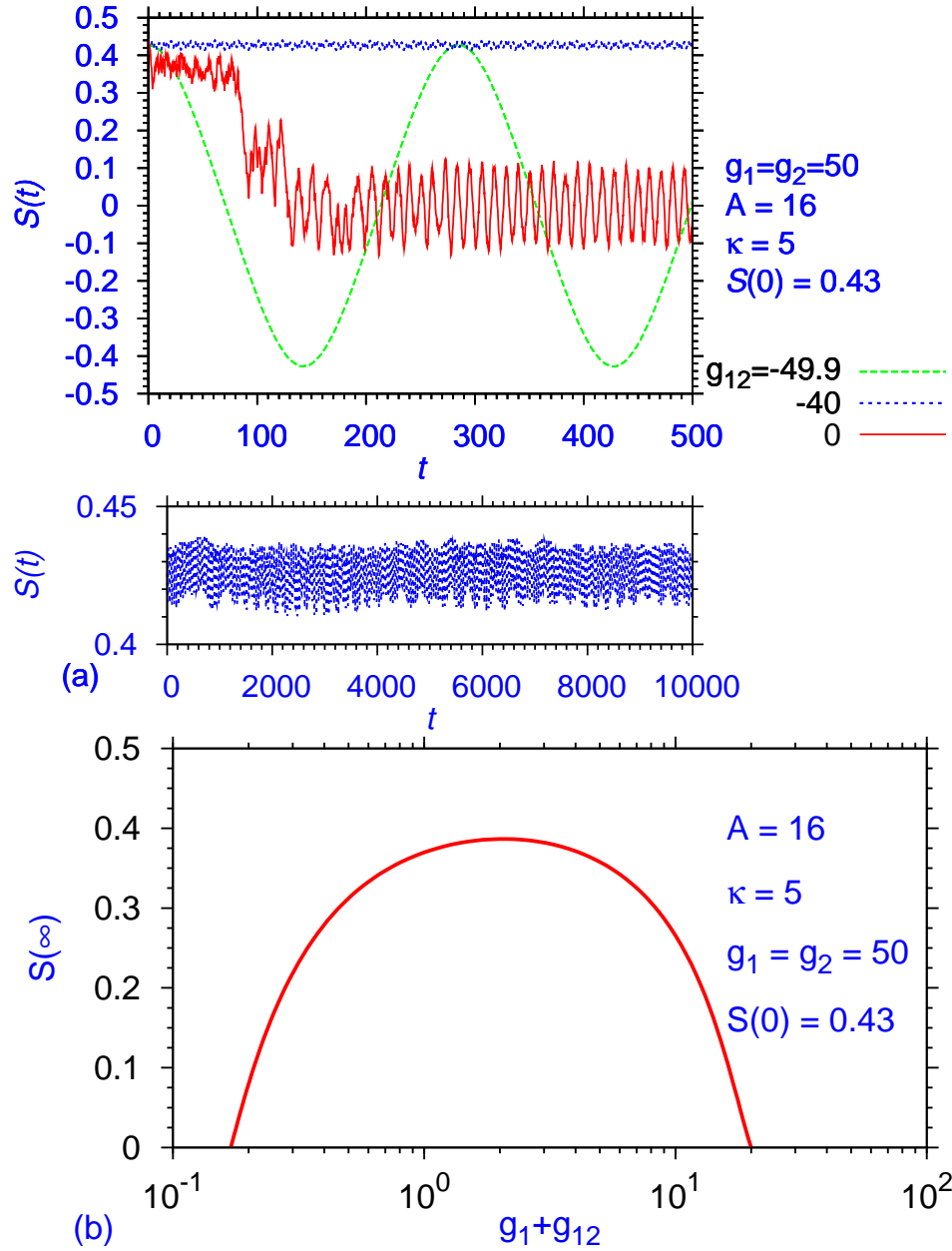


Figure 4. (a) (upper panel) Population imbalance $S(t)$ versus t for a binary BEC with $S(0) = 0.43$ and nonlinearities $g_1 = g_2 = 50$ and $g_{12} = 0, -40$ and -49.9 with DW (2). (lower panel) Long-time $S(t)$ versus t dynamics for $g_{12} = -40$. (b) Average population imbalance $S(\infty)$ at large time versus effective nonlinearity $g_1 + g_{12}$ for $S(0) = 0.43$.

3.2. Binary BEC

We consider the self trapping of a binary BEC in a DW for $g_i > g_{c2}$ and $g_i < g_{c1}$. In both cases no self trapping is possible for zero interspecies interaction ($g_{12} = 0$). Of these, for $g_i < g_{c1}$ we need a repulsive (positive) g_{12} to make both components sufficiently repulsive to have self trapping. But this case usually leads to a uninteresting stationary phase separated configuration [31] with the first species occupying the first well of the DW and the second species occupying the second well. A more interesting situation emerges for $g_i > g_{c2}$, when we require an attractive (negative) g_{12} to make both components appropriately repulsive to have self trapping. However, self trapping appears only for an intermediate $S(0)$ for an appropriate g_i and g_{12} . To illustrate, we consider the symmetric case with $g_1 = g_2 = 50$ in (1) and (2) and consider an attractive (negative) g_{12} . In the binary case, the self trapping is not so good for $\kappa = 10$, while the barrier between the two wells in (2) is narrow and we take $\kappa = 5$ in the numerical simulation. Permanent self trapping is found to occur for a narrow window of $S(0)$ around $S(0) = 0.4$. For $S(0) > 0.5$ and $S(0) < 0.3$ self trapping for a small interval of time could be obtained.

The initial state with $S(0) = 0.43$ for both components is created using DW (11) and reducing x_0 to zero. In the upper panel of figure 4 (a), we plot $S(t)$ versus t for both components for three values of g_{12} . For $g_{12} \geq 0$, no self trapping is possible and we are in the domain of irregular oscillation as shown for $g_{12} = 0$. For an attractive g_{12} , there is permanent self trapping as illustrated for $g_{12} = -40$. With further increase of $|g_{12}|$ the self trapping disappears and regular sinusoidal Josephson oscillation appears as shown for $g_{12} = -49.9$ in figure 4 (a). The lower panel of figure 4 (a) illustrates the population imbalance $S(t)$ for $g_{12} = -40$ at large times, which confirms robust self trapping. In figure 4 (b) we plot $S(\infty)$ for both components versus $g_1 + g_{12}$. In the symmetric case with $g_1 = g_2$, the wave function of the two components are equal and the quantity $g_1 + g_{12}$ is the effective nonlinearity of each component. Figure 4 (b) shows that self trapping occurs for the window of effective nonlinearity $0.2 < g_1 + g_{12} < 20$ for $S(0) = 0.43$. For any given initial population imbalance and for either sufficiently small or sufficiently large effective nonlinear interaction strength $g_1 + g_{12}$, the system is in the oscillation regime. For small values of effective interaction one has Josephson oscillation and for large values of effective interaction one has the classical center-of-mass oscillation. For intermediate interaction strength, the system may make transition to self trapping for an appropriate $S(0)$.

4. Analytical formulation for Optical-Lattice (OL) potential

For an OL, Eqs. (1) and (3) remain valid but with the variables bearing the following relations to the corresponding physical observables [24]: $t = (\pi/L)^2(\hbar/m)t_{\text{phys}}$, $x = \hat{x}\pi/L$, $V_0 = m(L/\pi\hbar)^2V_{ol}$, $\{g_i, g_{12}\} = (2NLm\omega_{\perp}/\pi\hbar)\{a_i, a_{12}\}$, where L the wavelength and V_0 the strength of OL potential: $V_{OL}(\hat{x}) = -V_0\pi^2\hbar^2/(mL^2)\cos(2\pi\hat{x}/L)$. The

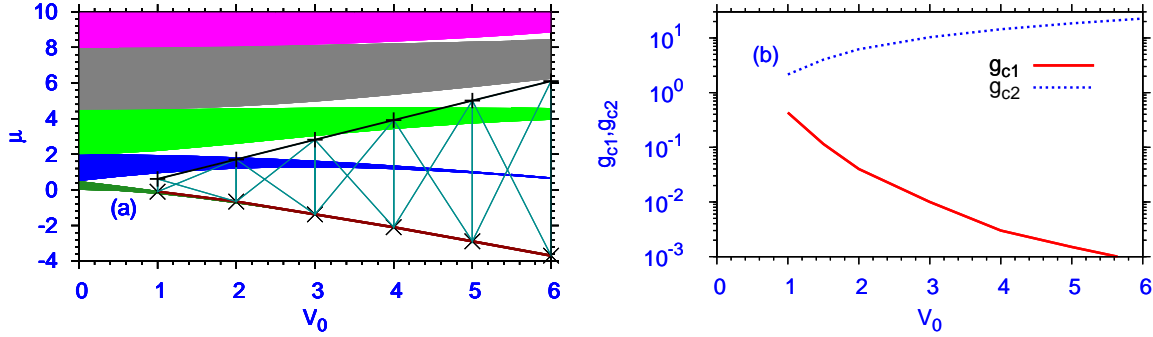


Figure 5. (a) Chemical potential μ versus V_0 showing the bands (shaded area) and gaps (white area) for OL (12). The hatched area between the lower line with crosses and the upper line with pluses represents the *variational* domain of the appearance of Gaussian gap solitons. The full white area above the lower line with crosses denote the *exact* domain of the appearance of gap solitons. (b) The critical values g_{c1} and g_{c2} defining the window of nonlinearities of Gaussian gap solitons versus V_0 .

dimensionless OL potential is given by

$$V(x) = -V_0 \cos(2x). \quad (12)$$

To critically examine the self trapping in a OL where the BEC is localized in one of the sites of the OL, we present a Gaussian variational analysis. The stationary state is described by (3) with the time derivative term $i\dot{\phi}$ replaced by $\mu\phi$ where μ is the chemical potential. The Lagrangian for that stationary equation is given by [19]

$$L = \int_{-\infty}^{\infty} \left[\mu\phi^2(x) - \phi_x^2(x)/2 - g\phi^4(x)/2 + V_0 \cos(2x)\phi^2(x) \right] dx - \mu. \quad (13)$$

This Lagrangian can be analytically evaluated by considering a simple form for the wave function ϕ . Using the Gaussian form [25] $\phi(x) = \pi^{-1/4} \sqrt{\mathcal{N}/w} \exp[-x^2/(2w^2)]$ with \mathcal{N} the norm and w the width, the Lagrangian can be written as

$$L = \mu(\mathcal{N} - 1) - \frac{\mathcal{N}}{4w^2} + V_0\mathcal{N} \exp(-w^2) - \frac{g\mathcal{N}^2}{2\sqrt{2\pi}w}. \quad (14)$$

The variational equations [25] $\partial L/\partial\mu = \partial L/\partial w = \partial L/\partial\mathcal{N} = 0$ yield $\mathcal{N} = 1$ and

$$1 + \frac{gw}{\sqrt{2\pi}} = 4V_0w^4 \exp(-w^2), \quad (15)$$

$$\mu = \frac{1}{4w^2} + \frac{g}{\sqrt{2\pi}w} - V_0 \exp(-w^2), \quad (16)$$

which determine the width and the chemical potential. We have set $\mathcal{N} = 1$ in (15) and (16) after derivation.

It is instructive to study the band and gap structure of the Schrödinger equation in the periodic OL potential (12): $\mu\phi(x) = -(1/2)\phi_{xx}(x) - V_0 \cos(2x)\phi(x)$ [26]. In a periodic potential the quantum excitation spectrum of a system consists of bands and gaps. The bands allow unlocalized plane wave solution modulated by a periodic function with the same period as the periodic potential known as Bloch wave. The gaps permit localized solution [26]. However, the single-particle linear Schrödinger equation does

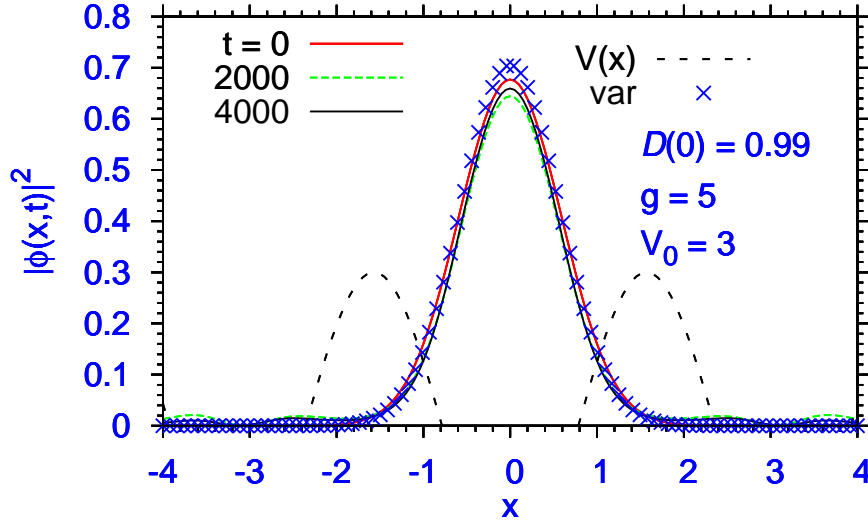


Figure 6. Density $|\phi(x,t)|^2$ versus x at different t when an initial Gaussian state with trapping measure $D(0) = 0.99$ is released at $x = t = 0$ on the OL. The variational result for the corresponding gap soliton is shown by crosses. The positive part of the potential is also shown in arbitrary units.

not allow any solution in the gap. The band (shaded regions) and gap (white regions above the lowest shaded region) of the spectrum of the Schrödinger equation with OL potential (12) is shown in figure 5 (a). The nonlinear 1D GP equation (3) for repulsive interaction (positive g) permits localized solutions in the gaps, called *gap solitons*, where the chemical potential μ lies in the gap. In the gaps, localized gap solitons are possible in the presence of an appropriate nonlinearity g .

We now find the condition for a gap soliton for a positive (repulsive) g by directly solving (15) and (16) for all g and V_0 . As μ tends to the upper edge of the lowest band, one has the lower limit g_{c1} of the formation of a gap soliton, denoted by a line with crosses in figure 5 (a). As the repulsive nonlinearity g is increased, (15) and (16) permit solution up to a maximum value g_{c2} which determine the upper limit of the formation of a gap soliton denoted by the line with pluses in figure 5 (a). The area between the two lines determine the domain in which the Gaussian gap solutions are allowed. (Gap solitons of non-Gaussian shape, possibly occupying many OL sites, are possible in the whole white region above the lowest band gap in figure 5 (a).) The nonlinearities corresponding to these two lines can be calculated using (15) and (16) and yields the critical g_{c1} and g_{c2} for self trapping. These nonlinearities are plotted in figure 5 (b).

5. Numerical results for Optical-Lattice (OL) potential

5.1. Single-Channel BEC

The numerical simulation is started by releasing a Gaussian state in the center of the OL during time evolution of the GP equation. The width of the Gaussian is taken such

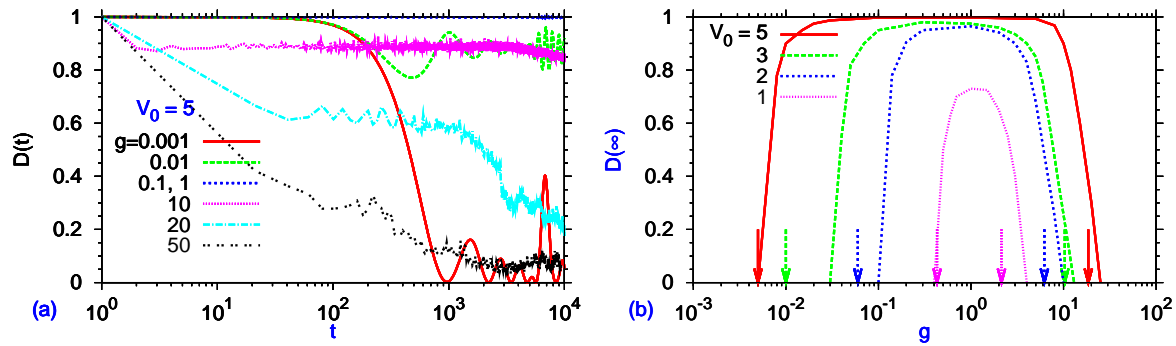


Figure 7. (a) Trapping measure $D(t)$ versus time t for $V_0 = 5$ for different g . (b) Trapping measure at large time $D(\infty)$ versus g for different $V_0 = 1, 2, 3, 5$. The respective arrows represent nonlinearities g_{c1} and g_{c2} from figure 5 (b).

that the initial state stays mostly in the central well of the OL. An estimate of self trapping is given by the following function called trapping measure

$$D(t) = \int_{-\pi/2}^{\pi/2} |\phi(x, t)|^2 dx. \quad (17)$$

Here we note that π is the wave length of the OL $-V_0 \cos(2x)$. Hence the function $D(t)$ determines the matter inside a single OL site. In case of ideal self trapping in a single site $D(t) = 1$, and $D(t)$ will tend to zero when self trapping is fully destroyed.

Self trapping occurs easily if the nonlinearity g is appropriate for a Gaussian gap soliton (viz. figure 5). We take an initial Gaussian state with $D(0) = 0.99$ and release it on the OL with $V_0 = 3$ and $g = 5$. The density profile of the trapped state are shown in figure 6. The small dispersion of the density profile at different t guarantees good self trapping. We also plot the density of the variational gap soliton, in good agreement with the self-trapped state, in figure 6.

In Fig 7 (a) we plot $D(t)$ versus t for $V_0 = 5$ and different g . For $g < 10$, $D(t)$ remains close to 1 for $t < 100$. However, if we continue to large t (< 10000) (a time much larger than the tunneling time of few hundred as in Fig 7 (a)), $D(t)$ remains close to 1 for a window of nonlinearity $0.01 < g < 10$ denoting permanent self trapping. For illustration, in figure 7 (b), we plot the trapping measure $D(t)$ at large times $D(\infty)$ versus g , where $D(\infty)$ is non-zero in the window $g_{c1} < g < g_{c2}$ corresponding to permanent self trapping and is zero outside showing no self trapping. In figure 7 (b) there are two arrows for each V_0 corresponding to g_{c1} and g_{c2} as obtained in figure 5 (b). The domain between the two arrows representing the region of allowed gap solitons (see, figure 5) agrees well with the domain of self trapping represented by non-zero $D(\infty)$ as seen in figure 7 (b). From this fact and also from the proximity of the variational solution for density of a gap soliton with that for the numerical self-trapped state in figure 6, we conclude that the self trapped state represents small oscillation of a stable gap soliton. In this connection, the finding in Ref. [13], that a self-trapped state in an OL is always temporary, is not fully to the point. They missed the fact that for the window of nonlinearity $g_{c1} < g < g_{c2}$ the self trapping could occur in a stable stationary

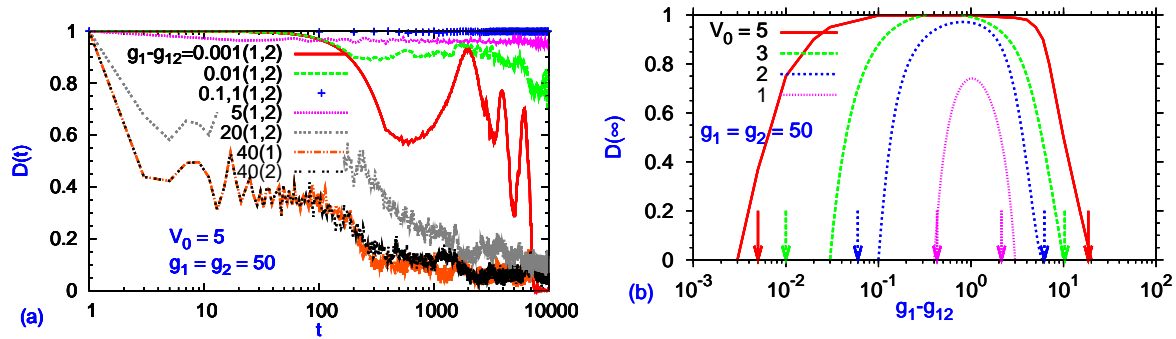


Figure 8. (a) Trapping measure $D(t)$ of a binary BEC versus time t for different $g_1 - g_{12}$. The curves are labeled by $g_1 - g_{12}$ and the component number in parenthesis. (b) Trapping measure at large time $D(\infty)$ versus $g_1 - g_{12}$ for different V_0 . The arrows are g_{c1} and g_{c2} from figure 5 (b).

gap soliton state leading to a permanent trapping. Just outside this small window of nonlinearity a temporary self trapping at small times may take place, as can be seen in figure 7 (a).

5.2. Binary BEC

To study self trapping of a binary BEC we consider large repulsive intraspecies nonlinearities $g_1 = g_2 = 50$, which do not allow self trapping for zero interspecies interaction $g_{12} = 0$ for $V_0 = 1, 2, 3, 5$, as seen in figures 7 (a) and (b). If we introduce an attractive (negative) interspecies interaction g_{12} , then in each channel the effective nonlinearity will be reduced and for a sufficiently large and attractive g_{12} one can have self trapping. The trapping dynamics for this system is illustrated in figure 8 (a) where we plot trapping measure $D(t)$ versus t for different g_{12} and $V_0 = 5, g_1 = g_2 = 50$. The results for the two components are practically the same in most cases. The self trapping appears for a small $(g_1 + g_{12}) (\approx 0.01)$ and disappears for large $(g_1 + g_{12}) (> 10)$. In this symmetric binary BEC, $(g_1 + g_{12})$ provides a good measure of the effective nonlinearity controlling self trapping. In figure 8 (b) we plot the trapping measure at large times $D(\infty)$ versus effective nonlinearity $g + g_{12}$ of the binary BEC for $V_0 = 1, 2, 3, 5$. The plots of figures 7 (b) and 8 (b) are qualitatively quite similar, showing that $(g_1 + g_{12})$ is a good measure of effective nonlinearity of the binary BEC. However, if $|g_{12}|$ is taken to be larger than g then the effective nonlinearity becomes attractive corresponding to a negative $g_1 + g_{12}$. This domain of nonlinearity corresponds to permanent symbiotic bright soliton [32] and consideration of self trapping is inappropriate.

Finally, we consider a binary BEC with small intraspecies nonlinearities and zero interspecies nonlinearity ($g_{12} = 0$), that does not allow self trapping, as found in figures 7 (a) and (b). As an illustration we consider the zero values for the intraspecies nonlinearities: $g_1 = g_2 = 0$. In the presence of appropriate repulsive interspecies nonlinearity ($g_{12} > 0$), one can have self trapping as illustrated in figures 9 (a) and (b). In figure 9 (a) we plot the trapping measure $D(t)$ versus t for different repulsive

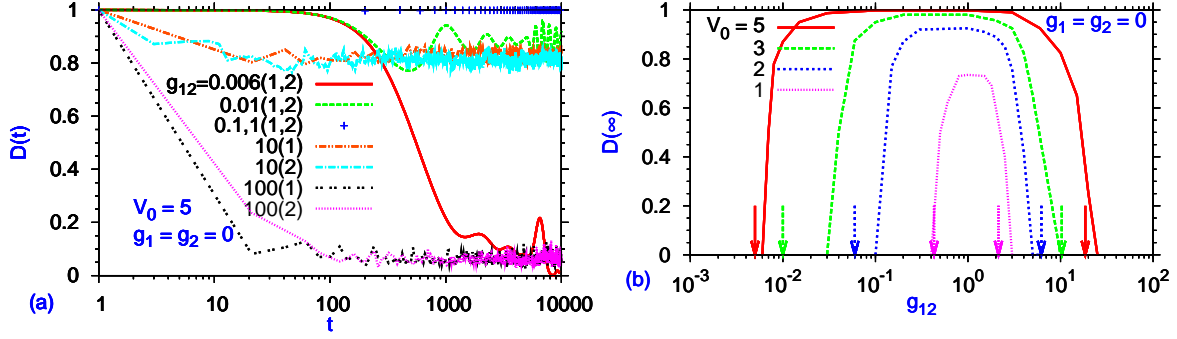


Figure 9. (a) Trapping measure $D(t)$ of a binary BEC versus time t for $V_0 = 5$ and different g_{12} . Curves are labeled by g_{12} and component number. (b) Trapping measure at large time $D(\infty)$ versus g_{12} for different V_0 . The arrows represent nonlinearities g_{c1} and g_{c2} from figure 5 (b).

(positive) interspecies nonlinearity g_{12} and $V_0 = 5, g_1 = g_2 = 0$. In this case g_{12} plays the role of effective interaction. There is a window of g_{12} values $g_{c1} < g_{12} < g_{c2}$ with $g_{c1} \approx 0.01$ and $g_{c2} \approx 10$, where permanent self trapping can be achieved. In figure 9 (b) we plot large-time trapping measure $D(\infty)$ versus g_{12} for different V_0 and $g_1 = g_2 = 0$. Qualitatively, this plot is quite similar to those in figures 7 (b) and 8 (b) showing the universal nature of these plots.

6. Summary and Discussion

We demonstrated that self trapping of a BEC or a binary BEC without interspecies interaction in OL and DW occurs for a window of repulsive intraspecies nonlinearity g ($g_{c1} < g < g_{c2}$), where g_{c1} and g_{c2} depends on the trap parameters. For a binary BEC with the intraspecies nonlinearities outside this window, a self trapping can be induced by a non-zero interspecies nonlinearity g_{12} such that the effective nonlinearities fall in this window. For intraspecies nonlinearities g_i below g_{c1} ($g_i < g_{c1}$), this is achieved by an appropriate repulsive (positive) g_{12} . For intraspecies nonlinearities g_i above g_{c2} ($g_i > g_{c2}$), one can have self trapping by introducing an appropriate attractive (negative) g_{12} . In case of self trapping in an OL, the permanently self trapped state represents breathing oscillation of a stable stationary gap soliton. On the other hand, the self trapping in a DW is purely a dynamical phenomenon without any underlying stationary state. However, the self trapping of a BEC and a binary BEC in both DW and OL could be permanent.

In previous studies of self trapping of a BEC, the existence of a lower limit g_{c1} of nonlinearity was noted [2, 7, 13, 14]. However, the disappearance of self trapping above an upper limit was not realized. (A similar upper limit appeared in a study of a Fermi superfluid in a DW [9].) In a previous study of self trapping in an OL, in contradiction with the present investigation, it was concluded that self trapping was always transient and should disappear at large t [13].

The principal findings of this critical study of self trapping are the following. (a)

The self-trapped states in an OL potential are essentially the stationary gap solitons. The self trapping in DW potential is entirely dynamical in nature and there are no stationary states in this case, such as the gap solitons of the OL potential. (There is no periodic potential and no band and band gap, specially for the case of a DW with a shallow barrier, which we shall study here.) It was generally believed that self trapping in both OL and DW potentials are dynamical in nature. (b) Self trapping is stopped beyond an upper limit of interaction in both cases. (c) In case of coupled systems with inter-species interaction self trapping is possible for domain of intra-species atomic interaction where no self trapping is allowed in uncoupled systems.

In the experiment of self trapping in an OL and in related theoretical studies a localized state over tens of OL sites [13, 14] was considered in contrast to that in predominantly a single OL site. Such states extended over multiple OL sites could possibly be a combination of multiple compact gap solitons. In another study, such states have been suggested to be a new type of spatially extended state in the gap [21]. The compact self trapped state on OL considered in this paper are different from the spatially extended states considered in other studies. Nevertheless, with the present experimental control over a BEC, it would be possible to study self trapping of the compact states on OL as considered in this paper.

Acknowledgments

FAPESP and CNPq (Brazil) provided partial support.

References

- [1] Görlitz *et al.* A 2001 *Phys. Rev. Lett.* **87** 130402
- [2] Albiez M, Gati R, Fölling J, Hunsmann S, Cristiani M and Oberthaler M K 2005 *Phys. Rev. Lett.* **95** 010402
Gati R and Oberthaler M K 2007 *J. Phys. B: At. Mol. Opt. Phys.* **40** R61
- [3] Kastberg A, Phillips W D, Rolston S L, Spreew R J C and Jessen P S 1995 *Phys. Rev. Lett.* **74** 1542
- [4] Roati G *et al.* 2008 *Nature* **453** 895
Khaykovich L *et al.* 2002 *Science* **256** 1290
- [5] Cataliotti F S *et al.* 2001 *Science* **293** 843
- [6] Javanainen J 1986 *Phys. Rev. Lett.* **57** 3164
Williams J E 2001 *Phys. Rev. A* **64** 013610
G Giovanazzi S, Smerzi A and Fantoni S 2000 *Phys. Rev. Lett.* **84** 4521
Adhikari S K 2005 *Phys. Rev. A* **72** 013619
Adhikari S K 2003 *Eur. Phys. J. D* **25** 161
Morales-Molina L and Gong J B 2008 *Phys. Rev. A* **78** 041403(R)
- [7] Smerzi A, Fantoni S, Giovanazzi S and Shenoy S R 1997 *Phys. Rev. Lett.* **79** 4950 (1997)
Trombettoni A and Smerzi A 2001 *Phys. Rev. Lett.* **86** 2353
Raghavan S, Smerzi A, Fantoni S and Shenoy S R 1999 *Phys. Rev. A* **59** 620
- [8] Ananikian D and Bergeman T 2006 *Phys. Rev. A* **73** 013604
Ottaviani C, Ahufinger V, Corbalán R and Mompert J 2010 *Phys. Rev. A* **81** 043621
Juliá-Díaz B, Dagnino D, Lewenstein M, Martorell J and Polls A 2010 *Phys. Rev. A* **81** 023615

- Lu L H and Li Y Q 2009 *Phys. Rev. A* **80** 033619
Martinez M T, Posazhennikova A and Kroha J 2009 *Phys. Rev. Lett.* **103** 105302
Shchesnovich V S and Trippenbach M 2008 *Phys. Rev. A* **78** 023611
Wang W, Fu L B and Yi X X 2007 *Phys. Rev. A* **75** 045601
Fu L B and Liu J 2006 *Phys. Rev. A* **74** 063614
Holthaus M 2001 *Phys. Rev. A* **64** 011601
- [9] Adhikari S K, Lu H and Pu H 2009 *Phys. Rev. A* **80** 063607
[10] Xiong B, Gong J, Pu H, Bao W and Li B 2009 *Phys. Rev. A* **79** 013626
[11] Milburn G J *et al.* 1997 *Phys. Rev. A* **55** 4318
[12] Liu B, Fu L-B, Yang S-P and Liu J 2007 *Phys. Rev. A* **75** 033601
[13] Wang B, Fu P, Liu J and Wu B 2006 *Phys. Rev. A* **74** 063610
[14] Xue J K, Zhang A X and Liu J 2008 *Phys. Rev. A* **77** 013602
Rosenkranz M, Jaksch D, Lim F Y and Bao W 2008 *Phys. Rev. A* **77** 063607
[15] Zhang W, Walls D F and Sanders B C 1994 *Phys. Rev. Lett.* **72** 60
Zhang W, Sanders B C and Tan W 1997 *Phys. Rev. A* **56** 1433
[16] Ostrovskaya E A *et al.* 2000 *Phys. Rev. A* **61** 031601(R)
[17] Billy J *et al.* 2008 *Nature* **453** 891
Adhikari S K and Salasnich L 2009 *Phys. Rev. A* **80** 023606
Adhikari S K 2010 *Phys. Rev. A* **81** 043636
Modugno M 2009 *New J. Phys.* **11** 033023
Cheng Y S and Adhikari S K 2010 *Phys. Rev. A* **81** 023620
Cheng Y S and Adhikari S K 2011 *Phys. Rev. A* **83**
Cheng Y S and Adhikari S K 2010 *Phys. Rev. A* **82** 013631
Cheng Y S and Adhikari S K 2010 *Laser Phys. Lett.* **7** 824
Larcher M, Dalfvo F and Modugno M 2009 *Phys. Rev. A* **80** 053606
- [18] Eiermann B *et al.* 2004 *Phys. Rev. Lett.* **92** 230401
Morsch O and Oberthaler M 2006 *Rev. Mod. Phys.* **78** 179
[19] Adhikari S K and Malomed B A 2007 *Europhys. Lett.* **79** 50003
[20] Ostrovskaya E A and Kivshar Y S *Phys. Rev. Lett.* **90** 160407
[21] Alexander T J, Ostrovskaya E A Kivshar Y S 2006 *Phys. Rev. Lett.* **96** 040401
[22] Zwierlein M W, Abo-Shaer J R, Schirotzek A, Schunck C H and Ketterle W 2005 *Nature* **435** 1047
- [23] Salasnich L, Parola A and Reatto L 2002 *Phys. Rev. A* **65** 043614
Muñoz Mateo A and Delgado V 2008 *Phys. Rev. A* **77** 013617 (2008)
Buitrago C A G and Adhikari S K 2009 *J. Phys. B: At. Mol. Opt. Phys.* **42** 215306
- [24] Adhikari S K and Malomed B A 2009 *Phys. Rev. A* **79** 015602
[25] PerezGarcia V M, Michinel H, Cirac J I *et al.* 1997 *Phys. Rev. A* **56** 1424
[26] Kittel C 1996 *Introduction to solid state physics, 7th Ed* (New York, Wiley)
[27] Muruganandam P and Adhikari S K 2009 *Comput. Phys. Commun.* **180** 1888
[28] Muruganandam P and Adhikari S K 2003 *J. Phys. B: At. Mol. Opt. Phys.* **36** 2501
Adhikari S K and Muruganandam P 2002 *J. Phys. B: At. Mol. Opt. Phys.* **35** 2831
[29] Adhikari S K and Salasnich L 2008 *Phys. Rev. A* **77** 033618
Adhikari S K and Salasnich L 2008 *Phys. Rev. A* **78** 043616
- [30] Sakmann K, Streltsov A I, Alon O E and Cederbaum L S 2009 *Phys. Rev. Lett.* **103** 220601
Zöllner S, Meyer H.-D. and Schmelcher P 2008 *Phys. Rev. Lett.* **100** 040401
Rigol M, Rousseau V, Scalettar R T and Singh R R P 2005 *Phys. Rev. Lett.* **95** 110402
- [31] Riboli F and Modugno M 2002 *Phys. Rev. A* **65** 063614
[32] Adhikari S K 2005 *Phys. Lett. A* **346** 179
Perez-Garcia V M and Beitia J B 2005 *Phys. Rev. A* **72** 033620